Arabian Journal of Chemistry (2023) **16**, 104423

King Saud University

Arabian Journal of Chemistry

www.ksu.edu.sa
www.sciencedirect.com

ORIGINAL ARTICLE

Optimization and evaluation of anticancer, antifungal, catalytic, and antibacterial activities: Biosynthesis of spherical-shaped gold nanoparticles using *Pistacia vera* hull extract (AuNPs@*PV*)

Mina Shirzadi-Ahodashti [a], Zirar M. Mizwari [b,c], Sarvin Mohammadi-Aghdam [d], Samin Ahmadi [e], Mohammad Ali Ebrahimzadeh [a,*], Sobhan Mortazavi-Derazkola [f,*]

[a] *Pharmaceutical Sciences Research Center, Hemoglobinopathy Institute and Department of Medicinal Chemistry, School of Pharmacy, Mazandaran University of Medical Sciences, Sari, Iran*
[b] *Department of Medical Laboratory Technology, Shaqlawa Technical College, Erbil Polytechnic University, Erbil, Iraq*
[c] *Rwandz Private Technical Institute, Erbil, Iraq*
[d] *Department of Chemistry, Payame Noor University, P.O. BOX 19395-3697, Tehran, Iran*
[e] *Student Research Committee, Faculty of Pharmacy, Mazandaran University of Medical Sciences, Sari, Iran*
[f] *Medical Toxicology and Drug Abuse Research Center (MTDRC), Birjand University of Medical Sciences, Birjand, Iran*

Received 2 August 2022; accepted 10 November 2022
Available online 15 November 2022

KEYWORDS

Gold nanoparticles;
Anti-cancer;
Anti-fungal;
Anti-bacterial;
Catalyst

Abstract In the past years, use of plant sources for the biosynthesis of nanoparticles has become very important. Gold nanoparticles with unique biological properties are one of these materials which are being investigated extensively. In the present study, the aqueous extract of *Pistacia vera* hull was utilized to fabrication of gold nanoparticles (AuNPs@*PV*) in a facile, environmentally friendly, and affordable way. Then the anticancer, antifungal, antibacterial, and photocatalytic potentials of AuNPs@*PV* were also investigated. The results of various techniques applied, including XRD, UV–vis, TEM, FT-IR, EDS, and FESEM showed the biological reduction of Au^{3+} ions to Au^{0}. Antibacterial studies were performed on a wide range of bacteria including seven strains of ATCC and seven strains of drug-resistant pathogens. According to the findings of this research, it seems that biosynthesized gold nanoparticles had good antibacterial activity against ATCC and drug-resistant strains of bacteria. The MIC values of *E. coli*, *S. aureus*, *P. mirabilis*, *P. aeruginosa*, *E. faecalis*, *K. pneumonia*, *A. baumannii* were 34.37, 4.2, 8.59, 4.29, 0.5, 34.37, and 8.59 μg/mL,

* Corresponding authors.
E-mail addresses: Zadeh20@gmail.com (M. Ali Ebrahimzadeh), S.mortazavi23@yahoo.com (S. Mortazavi-Derazkola).
Peer review under responsibility of King Saud University.

Production and hosting by Elsevier

https://doi.org/10.1016/j.arabjc.2022.104423

respectively. The result of the antifungal investigation showed that two pathogenic fungi, *Candida albicans* (IFRC1873) and *Candida albicans* (IFRC1874) were susceptible to AuNPs@*PV* with MIC values of 550 and 137 μg/mL, respectively. Furthermore, AuNPs@*PV* revealed noteworthy anti-cancer efficacy against AGS-3 and MCF-7 cell lines with IC_{50} values of 58.31 and 148.1 μg/mL, respectively. The results of the cytotoxicity effect of AuNPs@*PV* on BEAS-2B as a normal cell line indicated the selectivity of AuNPs@*PV* on cancerous cells. Furthermore, the fabricated AuNPs@*PV* under UV irradiation exhibited significant potential in the decolorization of methylene orange (MO) with a percent decolorization of 91.5 % after 20 min. Therefore, it can be concluded that biosynthesized gold nanoparticles as a photocatalyst, anti-bacterial, antifungal, and anti-cancer agents have potential applications in the fields of environment and biology.

1. Introduction

Nanotechnology is one of the most modern technologies in the world, which has unique and practical characteristics in the field of modern technology (like medicine (Mohammadzadeh et al., 2019; Khorsandi et al., 2022), pharmacology (Velsankar et al., 2022), and environment (Naghizadeh et al., 2021; Hashemi et al., 2022). Nanoscience is basically the ability to work at the molecular level to create new structures with the molecular organization (Khatami et al., 2018). It has been found that nanoparticles are very beneficial in the expansion and development of oral, transdermal, systemic, pulmonary, and other administration ways to investigate drug delivery, increase drug bioavailability and protect drug bioactivity. Owing to high surface-to-volume ratio of nanomaterials, these materials can penetrate cells and connective tissue without blocking capillaries. By encapsulating drugs with nanoparticles, it is possible to improve the absorption through the cell membrane, thus increasing the half-life of the drugs. Nanoparticles can also enter cancer cells as drug carriers and cause more drug penetration into the cancerous tumors. It has been reported several recent literature that some of the anti-tumor agents attached to nanoparticles display the long-term persistence of the drug in tumors, the reduction of tumor growth, and the long-term survival of tumor-bearing animals (Selvaraj and Alagar, 2007). Among various nanoparticles, our study is focused on gold nanoparticles due to their unique properties, including resistance to surface oxidation, chemical inertness, high stability, and multifunctional potential (Aljarba et al., 2022). These features led to the introduction of gold nanoparticles as an attractive option for drug delivery systems and nanoformulation (Eleraky et al., 2020). Also, gold nanoparticles have revealed potential applications for the delivery of antitumor agents, such as cisplatin and oxaliplatin via the detection of DNA. Gold nanoparticles can play an important role in effective antibacterial activities against some resistant strains due to photothermal properties and binding to surface ligands (Gubitosa et al., 2018). Expansion and clinical verification of new affordable therapeutic mechanisms against bacterial infections are urgently needed (Khan et al., 2016). Fungi cause many major diseases, including *Mycotoxicoses*, *Aspergillosis*, *Mycoses*, *Actinomycosis*, *Peniciliinosis*, *Candidiasis*, etc. The spherical gold nanoparticles from separate parts i.e., flower, bark, and the leaf of *Moringa oleifera* revealed the antifungal performance against *Aspergillus sp* at high concentration (Mondal et al., 2022). Despite the unique properties of nanoparticles, there is still space for further studies on antifungal, antimicrobial, and anticancer activities. On the other hand, one of the major concerns of people around the world is environmental pollution. These effluents lead to toxicity of industrial effluents. Therefore, they are considered a serious threat to the aquatic life system and human life (Shirzadi-Ahodashti et al., 2021). Different strategies, such as chemical methods, adsorption (Santoso et al., 2021; Li et al., 2018), and photocatalytic degradation (Ghoreishi, 2017; Shirzadi-Ahodashti et al., 2020; Ebrahimzadeh et al., 2019), exist for wastewater treatment. Among these, photocatalytic decomposition is one of the easiest and best techniques to destroy organic pollutions from sewage. Due to the reported photocatalytic applications of nanomaterials, the utilizing of these particles has increased in the past years (Samuel et al., 2020; Rani et al., 2020; Mani et al., 2020). A wide range of environmentally friendly nanoparticle synthesis approaches includes using enzymes and natural extracts (Singh et al., 2020). Among these, plant-mediated green synthesis is an eco-friendly, rapid, and simple process to synthesize metal nanoparticles (Ebrahimzadeh et al., 2020). Biomolecules in natural extracts (like flavonoids and phenol) play an essential role in reducing metal ions and converting them into nanoparticles (Fadaka et al., 2021). Recently, the extract of *Persicaria salicifolia* (Hosny and Fawzy, 2021); *Curcumae kwangsiensis* (Chen et al., 2021), and *Artemisia absinthium* (Keskïn et al., 2021) was applied in the synthesis of gold nanoparticles. In the present study, *P. vera* hull extracts were applied as stabilizing and capping agents for biosynthesis of gold nanoparticles (AuNPs@*PV*). *Pistachio* (*Pistacia vera* L.) belongs to the Anacardiaceae family and is native to the arid zones of Central and West Asia (Tomaino et al., 2010). The major pistachio-producing countries worldwide are Iran and Turkey. The hull of *P.vera* contains considerable antioxidant activity and natural biological mixtures (Moghaddam et al., 2009). Moreover, numerous reports displayed that the hull extract of *P. vera* possesses large amounts of polyphenolic compounds with several functions such as anti-inflammatory, anticancer, and antimicrobial. In addition, the hull extract of *P. vera* has properties such as preventing high blood pressure, anti-mutagenic and anti-diabetic (Seifzadeh et al., 2019; Arjeh et al., 2020; Behgar et al., 2011; Grace et al., 2016; Rajaei et al., 2010). In this study, the biological and photocatalytic activities of biogenic gold nanoparticles were investigated. For this purpose, extract of pistachio hull was applied for the fabrication of gold nanoparticles. It was investigated in terms of

anti-cytotoxic and anti-cancer activity against BEAS-2B, MCF-7, and AGS-3 cell lines for the first time. The antibacterial and antifungal performance of AuNPs@*PV* was measured against ATCC strains, resistant pathogens isolated from clinical, and eight fungal strains. Also, the efficiency of AuNPs@*PV* in removing the organic pollution methyl orange (MO) was examined. In the past years, studies have been conducted on the biological and catalytic activities of gold nanoparticles. There are some novelties of this study which are presented as follows. 1) Synthesis of gold nanoparticles using an environmentally friendly method and with the help of *P. vera* extract. 2) High biological activities (like antibacterial, antifungal, and anticancer). 3) Excellent photocatalytic pollutant decolorization under sunlight irradiation.

2. Experimental

2.1. Materials and chemicals used

The fresh hull of *P. vera* was gathered from the Rasht province of Iran and verified in the Sari Agriculture Sciences and Natural Resources University Herbarium. Methanol, 3-(4, 5-dimethylthiazol-2-yl)-2,5-diphenyltetrazolium bromide (MTT), chloroauric acid, and methyl orange (MO) were prepared from Sigma-Aldrich Company. Cisplatin was obtained from a pharmacy. Mueller Hinton agar was bought from Merck Company (Germany). BEAS-2B (human lung epithelial) as normal cell, MCF-7 (breast cancer), and AGS (human gastric cancer) as cancer cell lines were obtained from the Pasteur Institute of Iran. Bacterial strains were obtained from the Microbial collection of Iran, such as *Pseudomonas aeruginosa*, *Staphylococcus aureus*, *Proteus mirabilis*, *Acinetobacter baumannii*, *Klebsiella pneumonia*, *Enterococcus faecalis*, and *Escherichia coli*. The sources of antibiotic-resistant strains were procured from medical hospitals in Sari, Iran. The antifungal activity experiments were accomplished utilizing diverse fungal strains.

2.2. Extraction of P. vera

P. vera was extracted according to process described in a previous research with slight changes. 10 g of plant hull was washed with distilled water and then ground. Then, 100 mL of deionized water was added to 10 g of the plant at a temperature of 50 °C for 1 h. In order to separate the impurities, the waste material was separated using a filter.

2.3. Synthesis of AuNPs@PV

10 mL of extract of *P. vera* was added to $HAuCl_4{\cdot}3H_2O$ solution (10 mL and 1 mM). The reaction mixture was warmed to 50 °C with steady stirring until a change of color (yellow to purple-red). The reduction reaction was completed after 30 min. This color change indicates the formation of gold nanoparticles ($Au^{3+} \rightarrow Au^0$). A centrifuge (Centrifuge 5810R, Eppendorf, Germany) was used (6000 rpm and 20 min) to obtain gold nanoparticles. The obtained precipitate was washed with methanol and deionized water. Eventually, the final product was transferred to an oven (60 °C) for analysis and identification.

2.4. Antibacterial

The antibacterial performance of the AuNPs@*PV* were examined against Gram-positive (*E. faecalis* and *S. aureus*), Gram-negative (*P. mirabilis*, *A. baumannii*, *P. aeruginosa*, *K. pneumonia*, and *E.coli*) and seven multidrug-resistant pathogens isolated from clinical using the micro broth dilution assay. In order to obtain the minimum inhibition concentration (MIC), ATCC strains and resistant pathogens were cultured on MHA (Mueller Hinton Agar) medium for 24 h (37 °C). To get 10^7 CFU/mL of bacteria, the 0.5 McFarland suspensions was diluted at 1:10 in sterile normal saline. After, 100 μL of the prepared AuNPs@*PV* (550 μg/mL) were supplied to each well. Then, 100 μL of strain suspensions were added to each well.

2.5. Antifungal

In this examination, the MIC value was specified via the broth micro-dilution assay as defined in "method M27-A3 from the Clinical and Laboratory Standards Institute (CLSI) formerly NCCLS" (Alle et al., 2020). In this technique, 100 μL of AuNPs@*PV* was loaded to the first well. After dilution, 100 μL of cell suspensions were added to each well for two *C. albicans* strains (IFRC1874) and (IFRC1873), and 48 h for *T. mentagrophytes*, *A. fumigatus*, *T. mentagrophytes*, *F. equiseti*, *A. fumigatus*, and *F. proliferatum*.

2.6. Anticancer

2.6.1. Cell lines and cell culture

BEAS-2B cells and two AGS-3 and MCF-7 cell lines were grown in a DMEM media. The cell culture medium was enriched with penicillin/streptomycin and 10 % FBS and incubated in the presence of CO_2 (5 %; 37 °C). The concentration of Pen-Strep (penicillin/streptomycin solution) for cell culture was 1000 U/mL.

2.6.2. MTT assay for cell viability

The impact of AuNPs@*PV* on cell proliferation was assessed by MTT assay. 6–10 × 10^3 cells were counted and loaded into per well and incubated. All experiments were repeated three times to avoid errors. After 24 h, the cell culture supernatant was totally picked up and different concentrations of AuNPs@*PV* containing antibiotic and 10 % FCS were added to the culture media. The culture medium was the control. After 24 h incubations from the treatment of cell wells with various concentrations of AuNPs@*PV*, cell duplication was assessed. To characterize cell viability, MTT solution was added to each well and then incubated (4 h; 37 °C). To dissolve the purple crystals of formazan 100 μL of DMSO was added to each well, which shows cell viability. Eventually, the absorbance of the formazan was read from the ELISA plate reader (570 nm). Then the percentage of cell viability was calculated by comparing the control group.

2.7. Catalytic activity

The MO anionic dye decolorization as an indicator of AuNPs@*PV* photocatalytic activity was analyzed in the

presence of sodium borohydride under UV irradiation (400 W). The control solution consisted of 50 μL of 5 mM (MO), 2 mL of deionized water, and 100 μL of 0.1 M $NaBH_4$. Next, 50 μL of AuNPs@*PV* were added to the solution. The absorption spectra of the solution were monitored alternately by a UV–vis spectrophotometer. The decolorization percentage of pollutant was determined using following equation:

$$\text{Decolorizationrate}(\%) = (C_o - C_t/C_o) \times 100 \quad (1)$$

Where C_0 is the initial concentration and C_t is the concentration at time t.

2.8. Statistical analysis

Described analyses were carried out in triplicate. The statistical analysis was performed using a one-way analysis of variance (ANOVA) and the Duncan post-hoc test (P-value < 0.05).

2.9. Characterization

The UV–vis spectra of nanoparticles solution were determined using double beam spectrophotometer (Shimadzu, UV-2550, Kyoto, Japan). The particle size and shape of sample were investigated using transmission electron microscopy (TEM; Zeiss-EM10C-100 KV) and field emission scanning electron microscopy (FE-SEM; TESCAN BRNO-Mira3 LMU). Organic functional groups of dried *P. vera* hull and gold nanoparticles were measured in Perkin Elmer System 2000 FT-IR instrument. X–ray diffraction (XRD) measurement was carried out using Philips PW 1800 using a Cu Ka X–ray source.

3. Results and discussions

3.1. UV–Vis

The use of extract for the preparation of nanoparticles is one of the most widely used non-toxic, and environmentally friendly approaches. The functional groups in extracts can reduce metal ions and stabilize them (El-Seedi et al., 2019). In this study, employing a similar approach AuNPs@*PV* has been synthesized using the aqueous extract of, *P. vera* hull. The surface plasmon resonance (SPR) band of nanoparticles is one of the most characteristic features of nanomaterials (El-Borady et al., 2021). The phenomenon of SPR depends on various parameters such as the dielectric constant of the reaction mixture, size, morphology, and the aggregation conditions of the nanoparticles (Rahman et al., 2019; Taghavizadeh Yazdi et al., 2019). The color transformation of the reaction solution during heating from yellow to purple-red can be mainly attributed to the excitation of surface plasmon resonance (SPR) and is one of the critical pieces of evidence of the reduction of Au^{3+} ions to Au^0. This reduction was characterized by UV–vis (Shimadzu UV-1800) absorption spectroscopy. The most optimal temperature (room temp., 50 and 85 °C) for the synthesis of gold nanoparticles was investigated. As shown in Fig. 1, the presence of SPR bands around 500–800 nm confirmed the synthesis of AuNPs@*PV* stabilized by *P. vera* extract. According to the results, it is clear that the most optimal temperature is 50 °C.

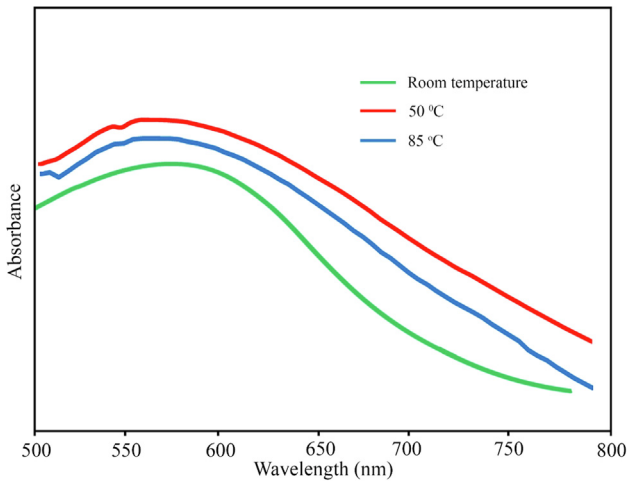

Fig. 1 The UV–Vis spectrum of gold nanoparticles.

3.2. High-performance liquid chromatography (HPLC)

HPLC was performed using a (C18) column (4.6 ×250 mm, 5 μm) (Shim-pack VP-ODS) and a binary solvent system (CH_3CN/H_2O and CH_3CO_2H). The standard solution (Fig. 2a) contained five phenolic compounds including cate-

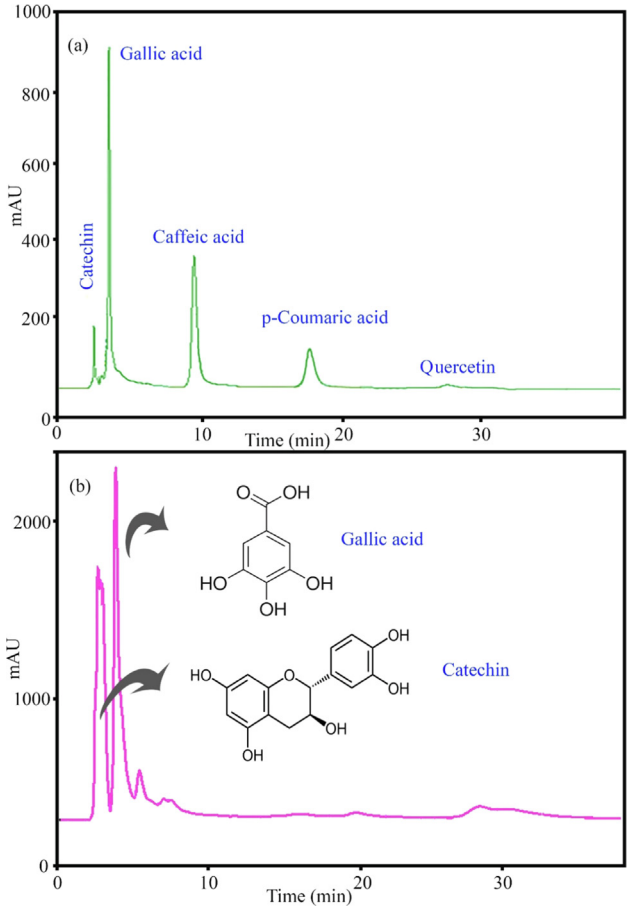

Fig. 2 HPLC chromatogram of (a) standard and (b) methanolic extract of *Pistacia vera* hull.

chin, gallic acid, caffeic acid, coumaric acid, and quercetin, which were separated in 40 min. The HPLC results (Fig. 2b) revealed that the main compounds in the *Pistacia vera* hull extract were catechin (4.1 mg/mL) and gallic acid (0.045 mg/mL). Based on HPLC results, the highest organic compound in *Pistacia vera* hull extract was catechin. The suggested mechanism for the synthesis of AuNPs has presented in Fig. 3. Catechin acts as a bidentate ligand and the protonation state of the catechol part plays an important role in the chelation of metal. Due to partial deprotonation in the initial oxidation stages, phenols are converted into o-quinones. Quinones act as capping agents that attach to gold nanoparticles via the negative charge of carbonyl groups. Electrons produced during the conversion of enol to quinonoid reduce Au^{+3} ions to gold atoms.

3.3. XRD

The crystalline nature and purity of AuNPs@*PV* were assessed by the XRD analysis (XRD; Philips X'pert PRO; Netherlands). AuNPs@*PV* illustrated four Bragg's diffraction patterns placed at 2θ angles: 38.20°, 44.22°, 64.79°, 77.67° which are related to (111), (200), (220), and (311). Accordingly, it suitable matches the face cubic structure of AuNPs (JCPDS card No 04–0784), as depicted in Fig. 4. Previous studies also report similar XRD patterns for synthesized gold nanoparticles (Ebrahimzadeh et al., 2020).

3.4. EDS, TEM and FESEM

The morphology and structure of AuNPs@*PV* were characterized by scanning electron microscopy, and the results are illustrated in Fig. 5. The intrinsic properties of nanoparticles rely on their size, shape and dispersion. It has also been proven that the high content of phenolic compounds surrounding the green synthesized nanoparticles leads to the creation of larger-sized particles (Rahman et al., 2019). FESEM and TEM micrographs (Fig. 5 a and b) revealed that the AuNPs@*PV* was mostly spherical-like morphology, homogeneous, and regular arrangement with a size ranging from 20 to 35 nm. Energy-dispersive X-ray spectroscopy (EDS) spectrometer as an elemental analytical technique was used to determine the purity and elemental compositions of products. The EDS spectrum of AuNPs@*PV* was illustrated in Fig. 6. Due to surface plasmon resonance, the AuNPs@*PV* revealed a typical optical absorption peak at ~3 KeV and other impurities are attributed to phytochemicals surrounding the surface of AuNPs@*PV* which leads to the stabilization of biosynthesized nanoparticles. The same result was acquired by Paul *et al.* (Paul et al., 2014), and Hamelian *et al.* (Hamelian et al., 2018).

3.5. FT-IR spectra

The FT-IR spectra of *Pistacia vera* hull extract and gold nanoparticles are shown in Fig. 7. The vibrational modes in the FTIR spectrum located at 3421, 2918, 1648, 1413, 1394, and 1065 cm^{-1}. The bands appear at 3421 cm^{-1} is related to the hydroxyl group of water molecules. The absorption bands at 1648, 1413, and 1065 cm^{-1} were ascribed to the stretching vibrations of -C═C–C group, stretching vibrations of -O-CH_3, and bending vibration of -C—O, respectively (Ebrahimzadeh et al., 2020).

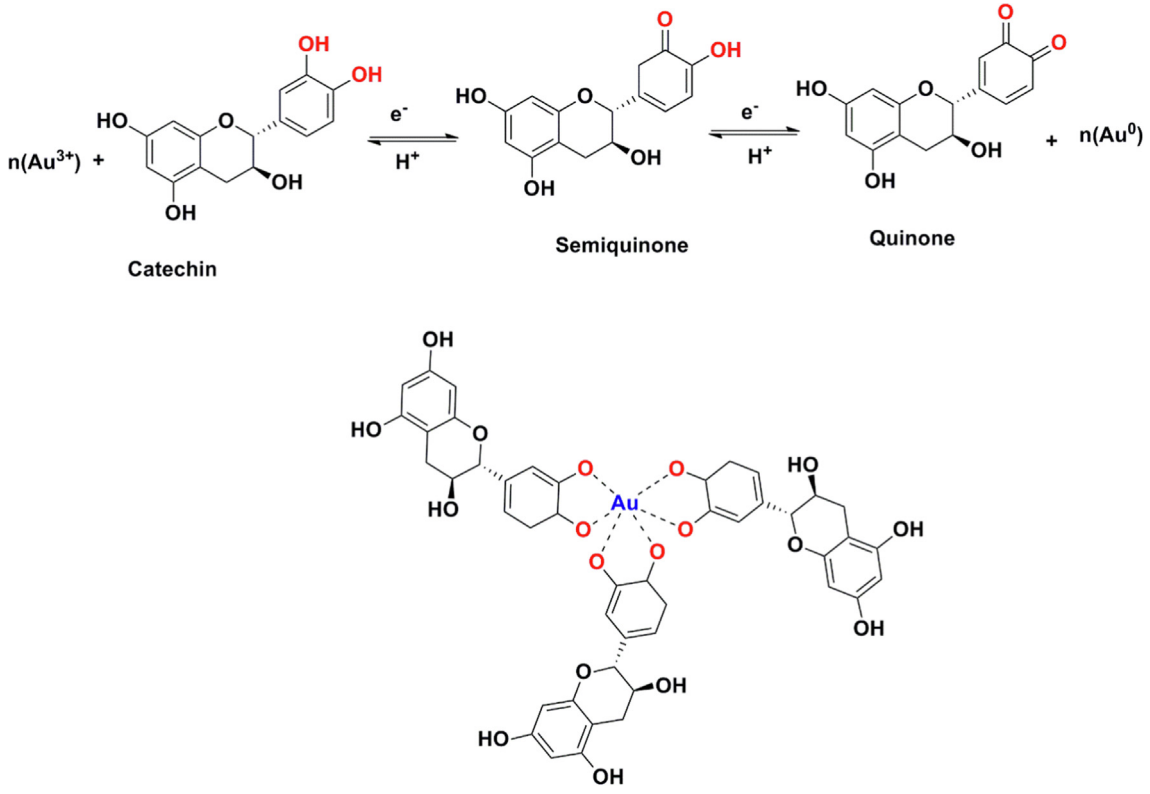

Fig. 3 The proposed reduction of gold ions with catechin for preparation of AuNPs@*PV*.

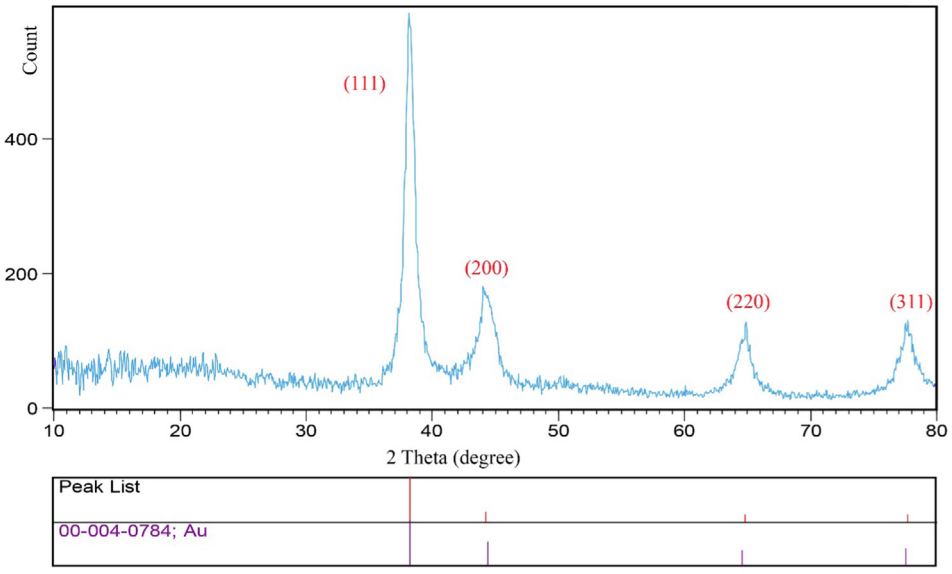

Fig. 4 XRD pattern of biosynthesized gold nanoparticles using *Pistacia vera* hull.

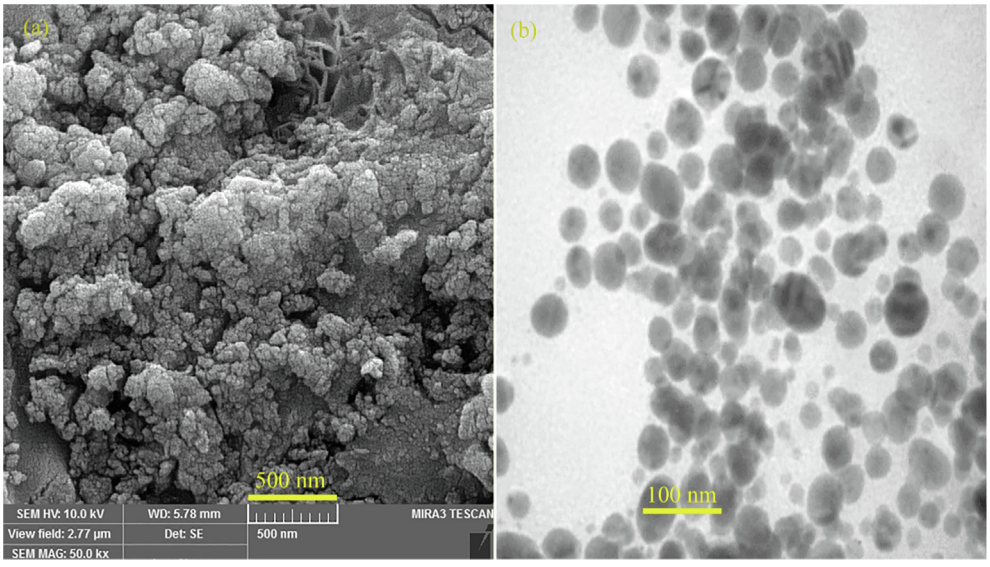

Fig. 5 (a) FESEM and (b) TEM image of biosynthesized gold nanoparticles using *Pistacia vera* hull.

3.6. Antibacterial activity

3.6.1. ATCC strains

This examination included seven ATCC strain bacteria. The result investigation of the antibacterial activity of AuNPs@*PV* compared to a standard antibiotic (ciprofloxacin) has been indicated in Table 1. The minimum inhibitory concentration of AuNPs@*PV* was observed for *E. faecalis* which was 0.5 µg/mL with MBC value of 2.14 µg/mL. As shown in Table 1, the value of MIC for both *S. aureus* and *P. aeruginosa* strains was equal to 4.2 µg/mL with MBC values of 34.37 and 137.5 µg/mL, respectively. The inhibition growth of *A. baumannii* and *P. mirabilis* by AuNPs@*PV* was seen in the concentration of 8.59 µg/mL as the MIC and 275 and 137.5 µg/mL as MBC. AuNPs@*PV* was capable to inhibiting the bacterial growth of *E. coli* and *K. pneumonia* strains with MIC values of 34.37 µg/mL with MBC values of 550 and 275 µg/mL, respectively. Because Gram-positives do not have an outer membrane, the penetration of nanoparticles into the bacterial cell is easier. Hence nanoparticles had a better effect on Gram-positives, including *E. faecalis*, and after that, *S. aureus*. *E. coli* and *K. pneumonia*, which had a higher MIC, are actually enterobacteria that are very resistant in terms of antibiotic resistance. Molecularly and genetically, they contain more resistance mechanisms in themselves. The results of studies on ATCC bacteria showed that AuNPs@*PV* has good potential antibacterial activity against Gram-negative and Gram-positive bacteria. Nanoparticle toxicity was reported to be raising the production of reactive oxygen species (ROS), and releasing metal ions inside the cells. Generally,

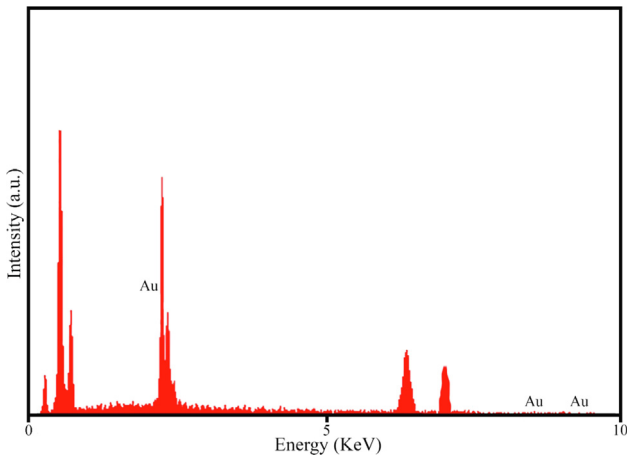

Fig. 6 EDS pattern of AuNPs@*PV*.

ROS production may affect oxidative stress and results in the blockage of a metabolic enzyme, and damage to DNA and cellular constituents. Hence, the nanoparticles with release metal ions, production of ROS, and ultimately inhibition of growth and cell division can lead to interference in a bacterial defense system and finally lead to the death of bacterial cells (Rahman et al., 2019; Manikandan et al., 2021).

3.6.2. Multi-drug resistance strains

The antibacterial performance of AuNPs@*PV* was examined against seven resistant strains of pathogens. The drug resistance of these pathogens was shown in a previous study (Hashemi et al., 2022). According to the information obtained, *S. aureus* isolated from the chip was resistant to all antibiotics but was sensitive to vancomycin. The prepared AuNPs@*PV* was able to inhibit the growth of *S. aureus* with MIC value of 34.3 μg/mL and 137.5 as MBC, respectively (Table 2). The MIC and MBC value of AuNPs@PV against *E. faecalis* was 68.7 μg/mL. *P. aeruginosa* and *A. baumannii* were immune to all the antibiotics documented in Table 2. Carbapenems are the last line of therapy, and MIC for colistin sulfate is reported to be 8 μg/mL and 256 μg/mL for *P. aeruginosa* and *A. baumannii*. In comparison, AuNPs@*PV* was able to inhibit their growth at 137.5 μg/mL as MIC, and 550 μg/mL as MBC for both strains. Separated *E. coli*, *K. pneumonia*, and *P. mirabilis* from urine were resistant to carbapenems and colistin. The minimum inhibitory and lethality concentrations of AuNPs@*PV* against *E. coli* and *P. mirabilis* were 68.7 μg/mL and 550 μg/mL for both strains. Both the MIC and MBC values of AuNPs@*PV* against *K. pneumonia* were 137.5 μg/mL. Gold nanoparticles are ideal drug carriers that can modulate the antibacterial effects of medicines and recreate an essential role in effective antibacterial approaches versus some resistant pathogens. It has been found that the antibacterial properties of gold nanoparticles functionalized with phytochemicals have a significant potential to overcome antibacterial resistance. Hence, various researchers aim to develop effective, environmentally friendly, and affordable gold nanoparticles to treat bacterial infections. Rajathi and his coworkers prepared gold nanoparticles utilizing *Stoechospermum marginatum* and evaluated their antibacterial activity against *Pseudomonas aeruginosa*, *Salmonella Typhimurium*, *Klebsiella oxytoca*, *Proteus vulgaris*, and *Klebsiella pneumonia*. Their finding demonstrated that synthesized gold nanoparticles have the highest activity on *Klebsiella pneumonia* among reported bacteria (Arockiya Aarthi Rajathi et al., 2012). Balasubramanian *et al.*, fabricated biogenic gold nanoparticles from the extract of *Jasminum auriculatum* and were observed that these nanoparticles have good antibacterial activity versus human pathogenic bacteria such as *E. coli*, *Klebsiella pneumonia*, *Streptococcus pyogenes*, and *S. aureus* (Balasubramanian et al., 2020). Gold nanoparticles have been synthesized from starch as a reducing agent and H_2O_2 as a reduction enhancer by Emam *et al.* Their antibacterial activity was examined against Gram-positive bacteria (*B. subtilis* and *S. aureus*) and Gram-negative (*P. aeruginosa* and *E. coli*). These nanoparticles

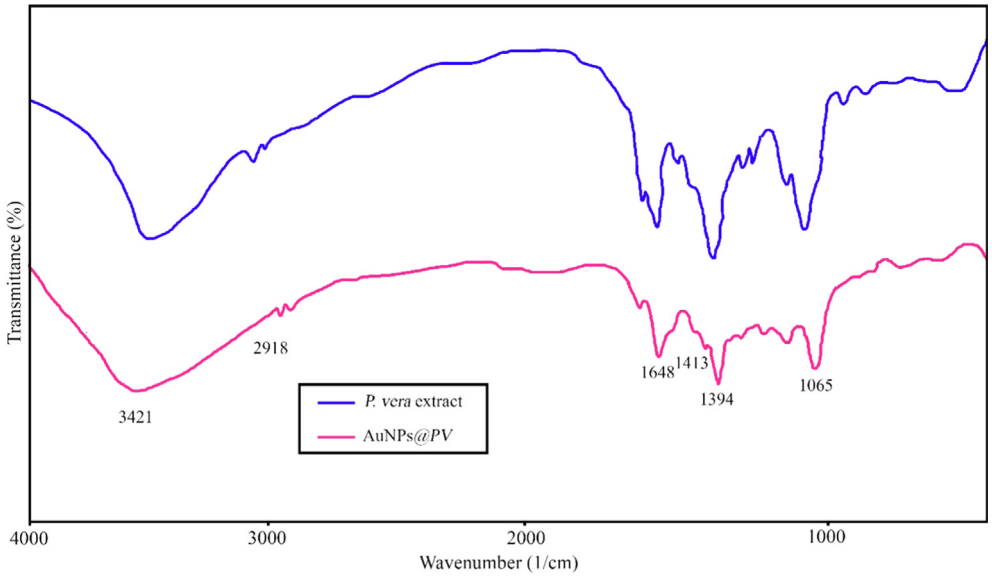

Fig. 7 FTIR spectrum of pure *Pistacia vera* hull and AuNPs@*PV*.

Table 1 Antibacterial activities of the synthesized gold nanoparticles against Gram-positive and Gram-negative bacteria.

Strains	AuNPs@*PV*		Extract	Ciprofloxacin
	MIC (μg/ml)	MBC (μg/ml)	MIC (μg/ml)	MIC (μg/ml)
S. aureus ATCC 2921	4.2	34.37	> 4000	0.21
E. faecalis ATCC 29212	0.5	2.14	> 4000	0.21
P. aeruginosa ATCC 27853	4.29	137.5	> 4000	0.3
A. baumannii ATCC 19606	8.59	275	> 4000	0.25
E. coli ATCC 25922	34.37	550	> 4000	0.1
K. pneumonia ATCC 700603	34.37	275	> 4000	0.1
P. mirabilis ATCC 25933	8.59	137.5	> 4000	0.1

Table 2 Antibacterial potential of the synthesized gold nanoparticles against multidrug-resistant isolates.

Strains	AuNPs@*PV*		Extract
	MIC (μg/ml)	MBC (μg/ml)	MIC (μg/ml)
S. aureus	34.3	137.5	> 4000
E. faecalis	68.7	68.7	> 4000
P. aeruginosa	137.5	550	> 4000
A. baumannii	137.5	550	> 4000
E. coli	68.7	550	> 4000
K. pneumonia	137.5	137.5	> 4000
P. mirabilis	68.7	550	> 4000

illustrated an excellent antibacterial effect on the strain of *S. aureus* at MIC value of about 960 μg/mL (Emam et al., 2017).

3.7. Antifungal activity

In this study, the antifungal performance of AuNPs@*PV* was evaluated by the standard microdilution procedure. The initial concentration of AuNPs@*PV* was 550 μg/mL. The results of the antifungal examination were illustrated in Table 3 and compared with itraconazole as a standard antibiotic. As shown in Table 3, all fungal strains except *Candida albicans* (IFRC1873) and *Candida albicans* (IFRC1874) were resistant to AuNPs@*PV*. The minimum inhibitory concentration of AuNPs@*PV* against *Candida albicans* (IFRC1873) and *Candida albicans* (IFRC1874) was 550 and 137 μg/mL, respectively. In a number of studies, the activity of gold nanoparticles as an antifungal has been investigated. In the studies of Mondal *et al.*, the spherical gold nanoparticles synthesized from several parts of the flower, bark, and leaf of *Moringa oleifera* displayed antifungal activity against the *Aspergillus sp* strain at the MIC value of 200 mg/L (Mondal et al., 2022). Lotfali & his coworkers studied the antifungal activity of gold nanoparticles against *Candida glabrata* fungal strains in the human vaginal tract. Their studies showed that

Table 3 The MIC value obtained from synthesized gold nanoparticles against different fungi isolated.

Fungi isolated tasted	AuNPs@*PV*	Extract	Itraconazole
	MIC (μg/ml)	MIC (μg/ml)	MIC (μg/ml)
Aspergillus fumigatus (IFRC 1649)	R	> 2500	≥16
Aspergillus fumigatus (IFRC 1505)	R	> 2500	≥16
Trichophyton mentagrophytes (FR1_22130)	R	> 2500	≥16
Trichophyton mentagrophytes (FR5_22130)	R	> 2500	≥16
Fusarium proliferatum (IFRC 1871)	R	> 2500	≥16
Fusarium equiseti (IFRC 1872)	R	> 2500	≥16
Candida albicans (IFRC1873)	550	> 2500	≥16
Candida albicans (IFRC1874)	137	> 2500	≥16

all these strains were resistant to amphotericin B, but they were sensitive to gold nanoparticles in the concentration range of 0.125 to 0.5 μg/mL (Lotfali et al., 2021). The result of Rautray and Rajananthini research in 2019 showed that the gold nanoparticles prepared by the mixture of extracts separated from *Pteris quadriureta* and *Adiantum capillus veneris* have good potential antibacterial against fungi like *Scedosporium apiospermum*; *Aspergillus niger*, *Aspergillus flavus*, *Trichophytonrubrum*, and *Aspergillus fumigates*. The MIC value of the gold nanoparticles on these strains was 50 mg/mL (Rautray and Rajananthini, 2020).

3.8. Anticancer activity

Cancer is a defect in the mechanisms of regulation of normal growth that led to uncontrolled cell growth, resistance to cell death, proliferation, ability to invade other tissues, and ultimately cell death (Khatami et al., 2018; Valsalam et al., 2019). In this study, the anti-cancer effect of AuNPs@*PV* was examined by MTT assay in the presence of cisplatin as the positive control. The concentration of cisplatin was 50 mg/mL. The IC_{50} of cisplatin against normal cell Beas-2B MCF-7, and AGS-3 was about 1.6, 4.95, and 6.3 μg/mL, respectively. The concentration of AuNPs@*PV* which reduces 50 % cell viability of AGS-3 and MCF-7 (IC_{50}), was observed at 58.31 and 148.1 μg/mL (Fig. 8). As can be seen in Fig. 8, cell death increases with increasing concentration of AuNPs@*PV*, and inhibition of 50 % cell viability needs a lower dose of nanoparticles. The therapeutic roles of NPs are due to their small size and unique coating, which can hold hydrophobic anticancer drugs in the exact location of the body. For this reason, they can reduce changes in the immune system. Despite gold nanoparticles' potential advantages for the treatment of many cancers, the application of Au-NPs is limited due to their incapacity to precisely target infected cells or cancerous cells

with a cytotoxic effect on both infected and healthy cells. The IC_{50} value of AuNPs@*PV* against normal cell was 455 µg/mL. Our previous research showed that a concentration of gold nanoparticles that led to the death of cancer cells did not have an inhibitory effect on the growth of normal cells. So, it can be concluded that nanoparticles acted selectively (Shirzadi-Ahodashti et al., 2020). Recently, Abd El-Moaty and his coworkers prepared gold nanoparticles using aerial parts of *Pituranthos tortuous* extract and evaluated their cytotoxic activity on human colon carcinoma (HCT-116) and Hepatocellular carcinoma (HepG-2) cell lines using the MTT assay. Their research showed that the growth of the HepG-2 and HCT-116 was inhibited by 5 to 15 nm spherical gold nanoparticles with an IC_{50} of 6.27 and 23.60 mg/mL, respectively (Al-Radadi, 2021). In another study by Mmola *et al*., biosynthesized spherical gold nanoparticles by *Algae Sargassum incisifolium* extract showed negligible toxicity against cancerous (HT-29 and MCF-7) and non-cancerous (MCF-12a) cell lines (Mmola et al., 2016). The anticancer activity of prepared spherical gold nanoparticles using *Backhousia citriodora* as a reducing agent against MCF-7 and HepG2 cancer cell line were studied by Khandanlou *et al*. The IC_{50} values against HepG2 and MCF-7 were reported as 108.21 and 116.65 µg/mL, respectively (Khandanlou et al., 2018).

3.9. Catalytic performance

The photocatalytic performance of AuNPs@*PV* for the decolorization of methyl orange (MO) was scanned under UV irradiation. Owing to the characteristic of localized surface plasmon resonance (LSPR) of AuNPs, these nanoparticles can be regarded as a potential photocatalytic agent for the destruction of industrial wastewater (Baruah et al., 2018). Factors that have a significant effect on the photocatalytic performance of nanoparticles and determine their physical, chemical, electronic, and optical properties include the surface charge of nanoparticles, morphology, and particle size (Ebrahimzadeh et al., 2020; Taghavizadeh Yazdi et al., 2019). The MO has a characteristic peak in the area at 480 nm; after the addition of AuNPs@*PV*, the orange color of MO disappeared after 20 min and subsequently, the maximum absorption intensity of MO slowly decreased, as depicted in Fig. 9a. In the absence of AuNPs@*PV*, no amount of MO was decolorized Fig. 9b. The methyl orange decolorization efficiencies by AuNPs@*PV* were estimated at around 91.5 %. In the studies of Fadaka & his coworkers, synthesized AuNPs using *Pimenta dioica* leaves aqueous extract was able to reduce the intensity of the methylene blue peak in the region of 664 nm within 2 min (Fadaka et al., 2021). El-Borady *et al*., synthesized gold nanoparticles by an eco-friendly method utilizing leaf extract of *Phragmites australis* and reported its photocatalytic activity on methylene blue. Their study showed that after the addition of biosynthesized gold nanoparticles the blue color of methylene blue disappeared after 1 min. The performance of this process can be attributed to the small size of gold nanoparticles, which leads to the creation of a large surface that helps the rapid transfer of electrons between $NaBH_4$ and MO and ultimately leads to the catalytic removal of MO (El-Borady et al.,

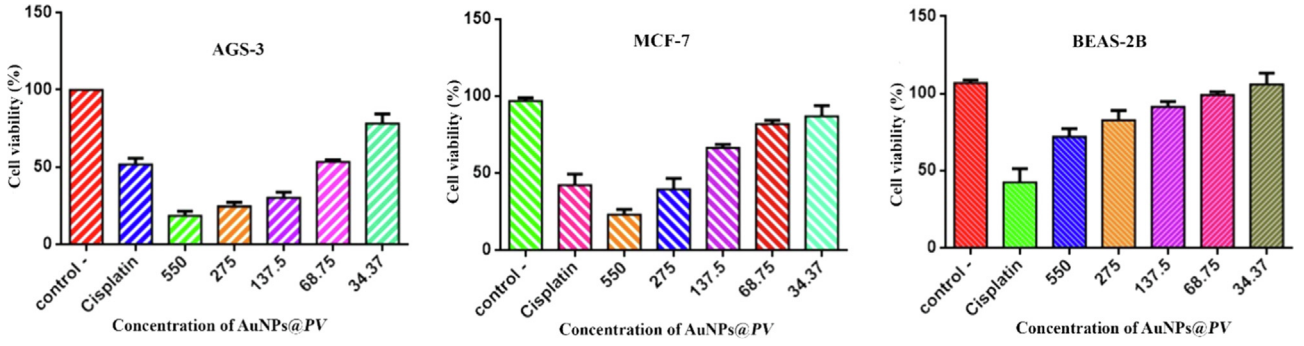

Fig. 8 Cytotoxicity analysis of biosynthesized gold nanoparticles on AGS-3, MCF-7 and BEAS-2B.

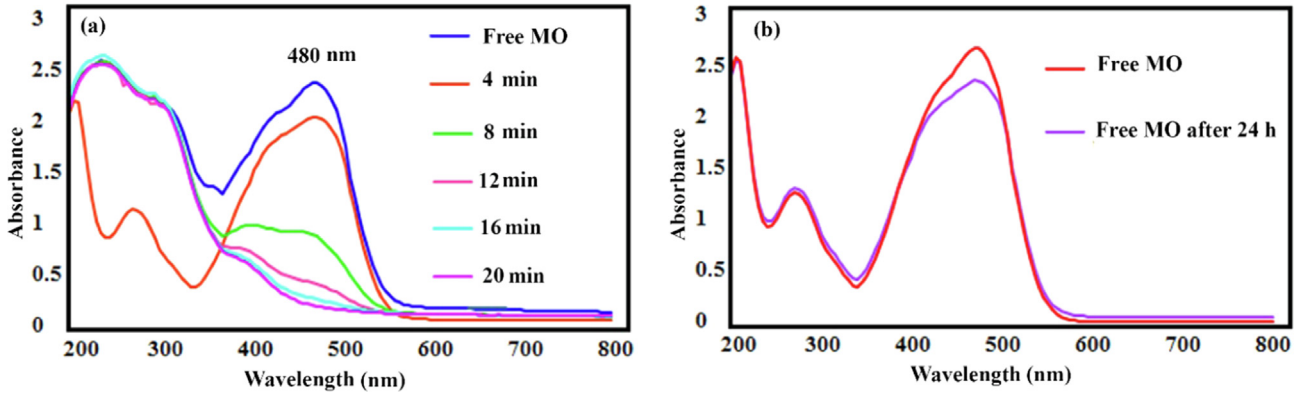

Fig. 9 (a) Catalytic activity of gold nanoparticles on methyl orange reduction; (b) in absence of gold nanoparticles.

2021). The results of the present study showed that the catalytic performance of AuNPs@PV was excellent, which was agreement with previous studies (Raj et al., 2020; Saravanan et al., 2017). The proposed mechanism of methylene blue dye decolorization using gold nanoparticles is described as follows:

$$\mathrm{AuNPs@}PV + \mathrm{UV}\,\mathrm{AuNPs@}PV^{*} + e^{-} \quad (2)$$

$$h^{+} + H_2O \rightarrow OH \quad (3)$$

$$e^{-} + O_2 \rightarrow O_2^{-} \quad (4)$$

$$OH + O_2^{-} + \mathrm{Dye} \rightarrow \mathrm{decolorization} \quad (5)$$

4. Conclusion

This research presents a simple, fast, and single-step procedure for bioreduction of Au^{3+} to Au^{0} to the biosynthesis of AuNPs using $HAuCl_4{\cdot}3H_2O$ and aqueous extract of *Pistacia vera* hull. The spherical morphology and the elemental composition of AuNPs@*PV* were determined by TEM, FE-SEM micrograph and EDS, respectively. The results of antibacterial studies showed that AuNPs@*PV* had a significant effect on ATCC bacterial and clinical-resistant pathogens strains. Moreover, AuNPs@*PV* displayed remarkable anticancer efficacy against AGS-3 and MCF-7 with IC_{50} values of 58.31 µg/mL and 148.1 µg/mL, respectively. The antifungal results showed that AuNPs@*PV* was able to inhibit the growth of *Candida albicans* (IFRC1873) and *Candida albicans* (IFRC1874) strains in quantities at 550 µg/mL and 137 µg/mL, respectively. In addition, the AuNPs@*PV* catalyzed the decolorization of the anionic dye (MO) with a percent of 91.5 % after 20 min under UV light irradiation. Hence, the present study demonstrated economical, effective, and multifunctional gold nanoparticles for improved catalytic and therapeutic applications.

Declaration of Competing Interest

The authors declare that they have no known competing financial interests or personal relationships that could have appeared to influence the work reported in this paper.

Acknowledgement

This study is the result of research number (code No. 9040). We express their gratitude to the Vice-Chancellor for Research at Mazandaran University of Medical Sciences for supporting this study.

References

Aljarba, N.H., Imtiaz, S., Anwar, N., Alanazi, I.S., Alkahtani, S., 2022. J. King Saud Univ. – Sci. 34, 101907.
Alle, M., Lee, S.-H., Kim, J.-C., 2020. J. Mater. Sci. Technol. 41, 168.
Al-Radadi, N.S., 2021. Arabian J. Chem. 14, 102956.
Arjeh, E., Akhavan, H.-R., Barzegar, M., Carbonell-Barrachina, Á.A., 2020. Trends Food Sci. Technol. 97, 55.
Arockiya Aarthi Rajathi, F., Parthiban, C., Ganesh Kumar, V., Anantharaman, P., 2012. Spectrochimica Acta Part A: Mol. Biomol. Spectrosc. 99, 166.
Balasubramanian, S., Kala, S.M.J., Pushparaj, T.L., 2020. J. Drug Delivery Sci. Technol. 57, 101620.
Baruah, D., Goswami, M., Yadav, R.N.S., Yadav, A., Das, A.M., 2018. J. Photochem. Photobiol., B 186, 51.
Behgar, M., Ghasemi, S., Naserian, A., Borzoie, A., Fatollahi, H., 2011. Radiat. Phys. Chem. 80, 963.
Chen, J., Li, Y., Fang, G., Cao, Z., Shang, Y., Alfarraj, S., Ali Alharbi, S., Li, J., Yang, S., Duan, X., 2021. Arabian J. Chem. 14, 103000.
Ebrahimzadeh, M.A., Mortazavi-Derazkola, S., Zazouli, M.A., 2019. J. Mater. Sci.: Mater. Electron. 30, 10994.
Ebrahimzadeh, M.A., Naghizadeh, A., Mohammadi-Aghdam, S., Khojasteh, H., Ghoreishi, S.M., Mortazavi-Derazkola, S., 2020. J. Photochem. Photobiol., B 209, 111949.
El-Borady, O.M., Fawzy, M., Hosny, M., 2021. Appl. Nanosci.
Eleraky, N.E., Allam, A., Hassan, S.B., Omar, M.M., 2020. Pharmaceutics 12.
El-Seedi, H.R., El-Shabasy, R.M., Khalifa, S.A.M., Saeed, A., Shah, A., Shah, R., Iftikhar, F.J., Abdel-Daim, M.M., Omri, A., Hajrahand, N.H., Sabir, J.S.M., Zou, X., Halabi, M.F., Sarhan, W., Guo, W., 2019. RSC Adv., 24539
Emam, H.E., Zahran, M.K., Ahmed, H.B., 2017. Eur. Polym. J. 90, 354.
Fadaka, A., Aluko, O., Awawu, S., Theledi, K., 2021. J. Multidisc. Appl. Nat. Sci. 1.
Ghoreishi, S.M., 2017. J. Mater. Sci.: Mater. Electron. 28, 14833.
Grace, M.H., Esposito, D., Timmers, M.A., Xiong, J., Yousef, G., Komarnytsky, S., Lila, M.A., 2016. Food Chem. 210, 85.
Gubitosa, J., Rizzi, V., Lopedota, A., Fini, P., Laurenzana, A., Fibbi, G., Fanelli, F., Petrella, A., Laquintana, V., Denora, N., Comparelli, R., Cosma, P., 2018. J. Colloid Interface Sci. 521, 50.
Hamelian, M., Hemmati, S., Varmira, K., Veisi, H., 2018. J. Taiwan Inst. Chem. Eng. 93, 21.
Hashemi, Z., Shirzadi-Ahodashti, M., Mortazavi-Derazkola, S., Ebrahimzadeh, M.A., 2022. Inorg. Chem. Commun. 139, 109320.
Hosny, M., Fawzy, M., 2021. Adv. Powder Technol. 32, 2891.
Keskïn, C., Atalar, M.N., Firat Baran, M., Baran, A., 2021. J. Institute Sci. Technol. 11, 365.
Khan, A.U., Wei, Y., Ahmad, A., Haq Khan, Z.U., Tahir, K., Khan, S.U., Muhammad, N., Khan, F.U., Yuan, Q., 2016. J. Mol. Liq. 215, 39.
Khandanlou, R., Murthy, V., Saranath, D., Damani, H., 2018. J. Mater. Sci. 53, 3106.
Khatami, M., Sharifi, I., Nobre, M.A., Zafarnia, N., Aflatoonian, M. R., 2018. Green Chem. Lett. Rev. 11, 125.
Khorsandi, Z., Hajipour, A.R., Sarfjoo, M.R., Varma, R.S., 2022. Mol. Catal. 532, 112701.
Li, Z., Sun, Y., Xing, J., Xing, Y., Meng, A., 2018. J. Hazard. Mater. 352, 204.
Lotfali, E., Toreyhi, H., Makhdoomi Sharabiani, K., Fattahi, A., Soheili, A., Ghasemi, R., Keymaram, M., Rezaee, Y., Iranpanah, S., 2021. Avicenna J. Medical Biotechnol. 13, 47.
Mani, M., Chang, J.H., Dhanesh Gandhi, A., Kayal Vizhi, D., Pavithra, S., Mohanraj, K., Mohanbabu, B., Babu, B., Balachandran, S., Kumaresan, S., 2020. Inorg. Chem. Commun. 121, 108228.
Manikandan, D.B., Sridhar, A., Krishnasamy Sekar, R., Perumalsamy, B., Veeran, S., Arumugam, M., Karuppaiah, P., Ramasamy, T., 2021. J. Environ. Chem. Eng. 9, 104845.
Mmola, M., Roes-Hill, M.L., Durrell, K., Bolton, J.J., Sibuyi, N., Meyer, M.E., Beukes, D.R., Antunes, E., 2016. Molecules (Basel, Switzerland) 21.
Moghaddam, T.M., Razavi, S.M., Malekzadegan, F., Ardekani, A.S., 2009. J. Texture Stud. 40, 390.
Mohammadzadeh, P., Shafiee Ardestani, M., Mortazavi-Derazkola, S., Bitarafan-Rajabi, A., Ghoreishi, S.M., 2019. IET Nanobiotechnol. 13, 560.

Mondal, A., Chowdhury, S., Mondal, N.K., Shaikh, W.A., Debnath, P., Chakraborty, S., 2022. Int. J. Environ. Sci. Technol. 19, 1573.
Naghizadeh, A., Mizwari, Z.M., Ghoreishi, S.M., Lashgari, S., Mortazavi-Derazkola, S., Rezaie, B., 2021. Environ. Technol. Innovation 23, 101560.
Paul, K., Bag, B.G., Samanta, K., 2014. Appl. Nanosci. 4, 769.
Rahman, A.U., Khan, A.U., Yuan, Q., Wei, Y., Ahmad, A., Ullah, S., Khan, Z.U.H., Shams, S., Tariq, M., Ahmad, W., 2019. J. Photochem. Photobiol., B 193, 31.
Raj, S., Singh, H., Trivedi, R., Soni, V., 2020. Sci. Rep. 10, 9616.
Rajaei, A., Barzegar, M., Mobarez, A.M., Sahari, M.A., Esfahani, Z. H., 2010. Food Chem. Toxicol. 48, 107.
Rani, P., Kumar, V., Singh, P.P., Matharu, A.S., Zhang, W., Kim, K.-H., Singh, J., Rawat, M., 2020. Environ. Int. 143, 105924.
Rautray, S., Rajananthini, A.U., 2020. BioPharm. Int. 33, 30.
Samuel, M.S., Selvarajan, E., Mathimani, T., Santhanam, N., Phuong, T.N., Brindhadevi, K., Pugazhendhi, A., 2020. J. Photochem. Photobiol., B 211, 112011.
Santoso, E., Ediati, R., Istiqomah, Z., Sulistiono, D.O., Nugraha, R. E., Kusumawati, Y., Bahruji, H., Prasetyoko, D., 2021. Microporous Mesoporous Mater. 310, 110620.
Saravanan, C., Rajesh, R., Kaviarasan, T., Muthukumar, K., Kavitake, D., Shetty, P.H., 2017. Biotechnol. Rep. 15, 33.
Seifzadeh, N., Ali Sahari, M., Barzegar, M., Ahmadi Gavlighi, H., Calani, L., Del Rio, D., Galaverna, G., 2019. Food Chem. 277, 398.
Selvaraj, V., Alagar, M., 2007. Int. J. Pharm. 337, 275.
Shirzadi-Ahodashti, M., Mortazavi-Derazkola, S., Ebrahimzadeh, M. A., 2020. Surf. Interfaces 21, 100697.
Shirzadi-Ahodashti, M., Ebrahimzadeh, M.A., Amiri, O., Naghizadeh, A., Mortazavi-Derazkola, S., 2020. Appl. Organomet. Chem. 34, e5467.
Shirzadi-Ahodashti, M., Hashemi, Z., Mortazavi, Y., Khormali, K., Mortazavi-Derazkola, S., Ebrahimzadeh, M.A., 2021. Colloids Surf., A: Physicochem. Eng. Aspects 617, 126383.
Singh, R.K., Behera, S.S., Singh, K.R., Mishra, S., Panigrahi, B., Sahoo, T.R., Parhi, P.K., Mandal, D., 2020. J. Photochem. Photobiol., A 400, 112704.
Taghavizadeh Yazdi, M.E., Modarres, M., Amiri, M.S., Darroudi, M., 2019. Res. Chem. Intermed. 45, 1105.
Tomaino, A., Martorana, M., Arcoraci, T., Monteleone, D., Giovinazzo, C., Saija, A., 2010. Biochimie 92, 1115.
Valsalam, S., Agastian, P., Esmail, G.A., Ghilan, A.-K.-M., Al-Dhabi, N.A., Arasu, M.V., 2019. J. Photochem. Photobiol., B 201, 111670.
Velsankar, K., Parvathy, G., Mohandoss, S., Ravi, G., Sudhahar, S., 2022. J. Drug Delivery Sci. Technol. 76, 103799.